Effects of the crystallite mosaic spread on integrated peak intensities in 2θ-ω measurements of highly crystallographically textured ZnO thin films

E. McCarthy[1], R.T. Rajendra Kumar[1,^], B. Doggett[1], S. Chakrabarti[1,$], R.J. O'Haire[1], S.B. Newcomb[2], J.-P. Mosnier[1], M.O. Henry[1], E. McGlynn[1,*]

[1] *School of Physical Sciences/National Centre for Plasma Science & Technology, Dublin City University, Glasnevin, Dublin 9, Ireland.*

[2]*Glebe Scientific Ltd., Newport, Co. Tipperary, Ireland.*

Abstract:

We report x-ray diffraction (2θ-ω and rocking curve) and transmission electron microscopy measurements on crystallographically textured ZnO thin films of varying thicknesses and crystallite mosaic spread deposited by pulsed laser deposition on Si. The integrated areas of the (0002) ZnO reflections in 2θ-ω mode do not scale with film thickness and in some cases show discrepancies of two orders of magnitude compared to expectations based solely on sample thicknesses. Intensity differences of this type are regularly used in the literature as indications of differences in sample crystallinity or crystal quality. However transmission electron microscopy data of our samples show no evidence of amorphous deposits or significantly varying crystal quality in different films. X-ray rocking curves of these samples do show substantial variations in the mosaic spread of crystallites in the ZnO films which are the origin of the differences in integrated

areas of the (0002) ZnO reflections in 2θ-ω measurements. We outline a generally applicable model to treat the 2θ-ω mode peak intensities which shows good agreement with the experimental data (to within an order of magnitude) and which is much simpler than utilizing a full reciprocal space map approach to understand the x-ray diffraction data. We conclude that the normalized integrated intensity of the (0002) ZnO reflection in highly crystallographically textured ZnO thin films is strongly dependent on the rocking curve width in addition to the film thickness and the use of such intensities in isolation as measures of the thin film crystallinity or crystal quality, without reference to the rocking curve width, is likely to be misleading when making judgments of such aspects of the thin film structure.

[*]Author to whom correspondence should be addressed: enda.mcglynn@dcu.ie.

[^]Present address: Department of Physics, Bharathiar University, Coimbatore 641 046, India.

[$]Present address: Department of Electrical Engineering, Indian Institute of Technology-Bombay, Powai, Mumbai 400 076, Maharashtra, India.

Introduction:

ZnO thin films have been the topic of extensive research in the past decade, with the aim of using the attractive photonic properties of the material in photonic devices such as LEDs and laser diodes [1]. The ubiquitous tendency of nominally undoped ZnO towards n-type conductivity has meant that reliable and reproducible p-type doping at carrier and mobility levels required for device operation has been extremely difficult to attain. Nevertheless, significant advances have been made in the quality of thin films grown by a number of techniques, including metal organic vapour phase deposition (MOCVD), molecular beam epitaxy (MBE) and pulsed laser deposition (PLD) [2]. In the majority of cases, the substrates used for ZnO thin film growth are either Si or one of the main sapphire planes (*c*-, *a*-, *m*- or *r*-planes). The growth is in the form of a columnar grain formation along the ZnO *c*-axis with the *c*-axis preferentially oriented normal to the substrate surface (i.e. showing crystallographic texture). This growth mode is reported even on amorphous substrates such as glass [3] and appears to be related both to the high basal plane surface energy of ZnO and also proximity effects of neighbouring columnar crystallites, which will tend to increase the *c*-axis crystallographic texture as the layer thickness increases, to reduce strain effects associated with the interaction / coalescence of non-normal columnar crystallites [4, 5]. The crystallographic texture is distinct from any surface texture (morphology) properties of the samples. We use the term "texture" solely in its crystallographic sense, in terms of preferred crystallite orientation.

X-ray diffraction (XRD) is an extremely useful workhorse technique in determining film parameters including strain, crystallinity/crystal quality, texture, coherence length and in-plane ordering [6]. A number of authors have recently used the peak intensity or integrated area of the (0002) ZnO reflection (or other reflections) as measures of the ZnO thin film crystallinity and/or crystal quality [7-11]. In this paper we report x-ray diffraction (2θ-ω and rocking curve) data on highly textured ZnO thin films of varying thicknesses deposited by PLD on Si, which show only ZnO (0002) and, occasionally, (0004) reflections (in addition to substrate peaks). The integrated areas of the (0002) ZnO reflections in 2θ–ω mode do not scale with film thickness and in some cases show discrepancies of two orders of magnitude compared to expectations based on sample thicknesses and could potentially be attributed to differences in sample crystallinity or crystal quality. However, transmission electron microscopy (TEM) data on our samples show no evidence of amorphous deposits or significant variations in crystal quality. We treat the problem in terms of the effects of mosaic spread on the reciprocal lattice spots, revealed by x-ray rocking curve data, and outline the effect of such mosaic spreads on the 2θ-ω mode peak intensities. We conclude by discussing the absolute necessity to account for rocking curve widths in discussions of the normalized integrated intensities of the (0002) ZnO reflection in highly textured ZnO thin films, especially when considering aspects such as thin film crystallinity or crystal quality.

Experimental Conditions:

The growth apparatus has been described in detail elsewhere [12, 13]. To summarise, ZnO thin films were deposited on Si (001) substrates using PLD by ablating a ZnO target (99.999%) in an oxygen atmosphere (99.999%, 75 mTorr) with a frequency quadrupled Nd:YAG laser (266 nm, 1.4 J/cm^2, 6 ns pulse duration, repetition rate 10 Hz). The Si substrates were degreased prior to growth and preheated *in-situ* at 950°C for 5 minutes. No effort was made to strip the native oxide. ZnO thin films with thicknesses in the range 30 – 1000 nm (determined by spectroscopic ellipsometry and corroborated by TEM measurements on certain samples) were then deposited, maintaining the substrates at 300° C and the ZnO films were then annealed in-situ at 700°C for 5 minutes. Different samples were grown at times many months apart. For spectroscopic ellipsometry data analysis following measurement either a two layer or a three layer stack model was used to achieve a best fit to the data. In the former case, a measurement of the bare silicon substrate with oxide was made and used as the substrate layer in the model, removing the need to add an oxide layer to the model. In this case ZnO was the second layer, with a variable thickness. In the latter case, a Si substrate with a silicon dioxide layer and a ZnO layer was used with variable thickness. A Forouhi & Bloomer dispersion formula was used for the ZnO layer with 2 oscillators and 8 parameters (and using standard parameter values for the ZnO layer). Roughness layers were tried in the model for a number of samples; however they were found to not improve the fit and typically returned thickness values of zero. Thickness values obtained from spectroscopic ellipsometry were compared against values obtained from surface profilometry measurements across step edges (using substrates where one half of the deposition region was masked during the PLD deposition) for a number of test samples and in all cases excellent agreement was

found. Furthermore, the agreement between thickness values from spectroscopic ellipsometry and cross-sectional TEM was excellent in all cases where comparisons were made.

The crystal structure was characterized by XRD (Bruker AXS D8 advance texture diffractometer). The XRD data in 2θ-ω mode were collected after careful optimization of the ω, ϕ and χ angles on the Si (004) reflection, to ensure comparability of the relative intensities (relative to the Si (004) reflection) of the ZnO (0002) reflection from sample to sample. The ϕ angle has been adjusted in some cases to reduce or eliminate the kinematically forbidden Si (002) reflection which is seen through double diffraction effects [14]. Rocking curve data were also collected for these samples (in addition to a limited number of ϕ scan measurements). Because of the extended period over which samples were grown significant variations in diffractometer x-ray output intensity were observed, so in all cases where comparisons are being made we use only (integrated) intensities suitably normalized to the Si substrate peak integrated intensity. Samples for TEM characterisation were thinned to electron transparency using standard focused ion beam milling procedures [15] and examined in a JEOL2000FX operating at 200kV.

Results and Discussion:

Figure 1(a) shows XRD diffractograms in 2θ-ω mode on four representative ZnO samples, i, ii, v and vi as listed in table 1 while figure 1(b) shows rocking curve data for the same samples. The rocking curves are fitted with a Gaussian lineshape, including a

baseline offset, to determine the peak widths and the fit lines are shown in the figure. The small features marked "A" are due to the plastic-backed adhesive tape used to mount the samples, while the features marked "B" are due to K_β radiation from the x-ray tube at ~ 62^0 and tungsten L_α radiation from contamination of the x-ray tube at ~ 66^0 [16]. Changes in the central maximum position in figure 1(b) are due to (small) random sample tilts during the sample mounting procedure.

The 2θ-ω data show that the samples are highly textured ZnO, with significant contributions only from the ZnO (0002) planes (and occasionally the 2^{nd} order (0004)) and Si (004) planes. In one case (sample v) a small reflection due to the kinematically forbidden Si (002) reflection is seen also [14]. The samples show some evidence of slight strain, varying from sample to sample (and is least in thicker samples), but in all cases the measured strain is much less than 1%. The integrated intensities for all eight samples (after subtraction of background intensities) of the ZnO (0002) and Si (004) peaks are listed in table 1, in addition to the rocking curve full widths at half maximum (FWHM). The rocking curve widths were found to be independent of the sample ϕ angle in all cases. Table 1 also lists other key sample properties such as thickness (as determined by spectroscopic ellipsometry and corroborated for some samples by cross-section TEM data).

Table 1 (column 6, boldfaced) shows that the normalized integrated intensity (with respect to the Si (004) peak integrated intensity) per nm of the samples varies over a range of almost two orders of magnitude. As mentioned previously, a number of authors

have recently used the peak intensity or integrated area of the (0002) ZnO reflection in isolation as measures of the thin film crystallinity [7-11]. The results shown in table 1 based on the data in figure 1(a) would, if taken as a measure of film crystallinity, imply a significant difference in the crystalline to amorphous deposit ratio in our samples. However, the cross-sectional TEM data shown in figures 2 and 3 for the samples labelled (ii) and (v) in figure 1 and table 1, respectively reveal a crystallographically textured deposit in the form of columnar crystallites with their long axes lying mainly perpendicular to the substrate. The contrast variations seen in dark field micrographs (imaged using the (10-10) ZnO reflection) shown in figures 2(c) and 3 (c) are similarly fully consistent with the presence of a textured polycrystalline deposit and further emphasise that no amorphous oxide has been formed. These observations are similar to other reports for ZnO layer growth in Si substrates with a native oxide [3] and also confirm the spectroscopic ellipsometry measurements for both 40 nm and 425 nm layer deposits. XRD rocking curves shown in figure 1(b) however reveal substantial sample to sample variations in the degree of texture of the samples, with smaller rocking curve widths generally found in thicker samples, but with variations from this trend also present. The origin of this variation is due to (a) changes in film thickness, which lead, due to proximity effects of neighbouring crystallites, to changes in texture (generally smaller mosaic spread for thicker films) [5] and (b) small variations in growth parameters over the extended time period over which the sample set was grown, which are known to also affect sample texture [3].

The normalized (per unit volume of material) intensity of an XRD reflection in θ-2θ or 2θ-ω modes corresponding to a change in x-ray wavevector k is proportional to the absolute value squared of the Fourier transform of the x-ray scattering density with respect to k in the regime of kinematic diffraction appropriate for the thin, polycrystalline mosaic ZnO films studied here [6, 17]. For these samples the scattered intensity is spread over a range of k values centred on the reciprocal lattice points of the perfect single crystal because of (a) the effects of finite coherence length of the individual crystallites and (b) the mosaic spread of the crystallites [6]. The integral of the scattered intensity over this range in reciprocal space which gives a total intensity for reflections from this set of planes is proportional to the sample volume [6, 17, 18]. One can envisage this for the samples discussed here in the form of a density plot in k-space, with the density representing the normalized scattered intensity at that value of k, as shown schematically in figure 4. In figure 4 the shading of the (oblate spheroidally-shaped) reciprocal lattice spot indicates that this density and the size in various directions is a measure of the spread of the spot in reciprocal space (e.g. its FWHM). The spread of the spot in the direction normal to the sample surface ($k_{\perp}$) is determined by the out-of-plane coherence length of the crystallites (Scherrer formula [6]), while its extent in a direction parallel to the sample surface ($k_{||}$) is predominantly determined in these samples by the mosaic spread of the crystallites (as measured by the rocking curve FWHM) [6, 18]. For a fixed thin film volume, the greater the mosaic spread the larger the volume of reciprocal space over which the scattered intensity is distributed and, since the total integrated density is proportional to the film volume, this implies that the peak density reduces at a rate inversely proportional to the square of the rocking curve FWHM (if, as in this case, it is

independent of ϕ). The 2θ-ω mode of operation essentially scans through reciprocal space in a direction normal to the substrate surface ($k_{\perp}$) and thus measures the intensity along such a trajectory in k-space, while a rocking curve scans through reciprocal space in a direction parallel to the substrate surface ($k_{||}$) [18]. These points are shown schematically in figure 4, for examples of small (4(a)) and large (4(b)) mosaic spreads in a textured thin film of constant volume and constant out of plane coherence length (the shading of the ZnO (0002) reciprocal lattice spot on the left hand side indicates the normalized scattering density/intensity). Schematic representations (with indicative intensity and angular scales for comparative purposes) are shown for 2θ-ω and rocking curve scans of the two situations on the right hand side of figure 4. Hence the integrated intensity of the symmetric film reflections for a highly textured film in 2θ-ω mode should be proportional to the sample volume (film thickness) and inversely proportional to the rocking curve FWHM squared, or equivalently, the product of the rocking curve FWHM squared and the integrated normalized intensity should be proportional to film thickness. The use of integrated 2θ-ω intensities removes any variation due to changes in the out of plane coherence length from sample to sample.

In Table 1 the product of the rocking curve FWHM squared multiplied by the integrated normalised intensity per nanometer oxide layer thickness is shown in column 8 (boldfaced and italicised), and it is seen that, in contrast to column 6, the values for all samples are of the same order of magnitude (with an average value of 2.21×10^{-3} and a standard deviation of 0.55×10^{-3}), which is consistent with the model outlined above (the sources of the remaining spread of values/discrepancies are briefly discussed below). It is

clear that variations in rocking curve FWHM are responsible for substantial discrepancies (up to two orders of magnitude) in the normalized integrated intensity per nm of the (0002) peak for ZnO thin films and that these discrepancies are largely reconciled when variations in FWHM are taken into account with the model above. We note that the approach outlined above is suitable for analysis of highly textured thin films, such as those in our case which display a single lattice plane reflection (and higher orders of same). It will become less useful (and ultimately redundant) as the degree of texture reduces and different lattice plane reflections appear in the diffractogram (until finally the powder pattern is recovered when the texture vanishes).

The remaining spread in values in our data in column 8 of table 1 is primarily due to the practical difficulties encountered in normalizing with respect to the Si (004) peak integrated intensity. The sample orientation was optimized by adjusting the ω, ϕ and χ angles on the Si (004) reflection to achieve maximum intensity. However, the very low FWHM of this peak in angular terms (the rocking curve FWHM for Si (004) was measured as $\sim 0.06^0$, data not shown) means that slight mis-adjustments due to the finite step size of the instrument and the sequential nature of angular optimizations can cause changes (~ 10's of %) in the Si (004) peak intensity in the 2θ-ω mode, which account for the majority of the remaining discrepancy in column 8. In fact, for samples measured in similar conditions on the same day on the same instrument (where the x-ray intensity is unlikely to change greatly) it is probably more accurate to use the unnormalised ZnO (0002) integrated intensity. However, when seeking to compare samples grown over extended time periods during which the x-ray source intensity may have changed (as in

the present study), or where the measurement conditions have changed substantially, normalization with respect to the Si (004) integrated intensity is necessary.

Conclusions:

The normalized integrated intensity of the (0002) ZnO reflection in highly textured ZnO thin films is strongly dependent on the rocking curve FWHM in addition to the film thickness and the use of such intensities "in isolation" as measures of the thin film crystallinity or crystal quality, without reference to the rocking curve FWHM, is likely to be misleading in any assessment of these aspects of the thin film structure. We have outlined a model which shows that the product of the rocking curve FWHM squared and the integrated normalized intensity should be proportional to film thickness and this prediction compares very well with XRD data from a range of samples of varying thicknesses and degrees of mosaic spread deposited by pulsed laser deposition on Si. The remaining discrepancy is explained by the difficulty of normalizing to the very sharply defined Si (004) XRD peak. In recent times a number of reports on potential complexities and pitfalls in XRD characterization of thin film and nanostructured materials have appeared [14, 19]. While the points discussed above have been recognised by the crystallography community for many years [20], they seem to be less well known among the thin film community and thus this note may be useful to re-emphasize them.

Acknowledgements:

The authors gratefully acknowledge financial support from Science Foundation Ireland (Investigator Grant # 02/IN1/I95) and the Irish Higher Education Authority under the NDP. RTRK and EMcG also wish to acknowledge the International Visitors Programme of DCU which provided a fellowship for RTRK to visit DCU in the summer of 2010. We are grateful to Dr. Barry O'Connell and Mr. Henry Barry (DCU) for their assistance in performing ellipsometry measurements.

References:

[1] Ü. Özgür, Ya. I. Alivov, C. Liu, A. Teke, M. A. Reshchikov, S. Dogan, V. Avrutin, S.-J. Cho and H. Morkoç, J. Appl. Phys. **98**, article #041301 (2005).

[2] L.W. Martin, Y.-H. Chu and R. Ramesh, Mat. Sci. Eng. R **68** 89 (2010).

[3] J.-I. Hong, J.-H. Bae, Z.L. Wang and R.L. Snyder, Nanotechnology **20** article #085609 (2009).

[4] L.E. Greene, M. Law, D.H. Tan, M. Montano, J. Goldberger, G. Somorjai and P.D. Yang, Nano Lett. **5**, 1231 (2005).

[5] B. Postels, M. Kreye, H.-H. Wehmann, A. Bakin, N. Boukos, A. Travlos and A. Waag, Superlatt. Microstruc. **42** 425 (2007).

[6] B.D. Cullity and S.R. Stock, Elements of X-Ray Diffraction, 3rd Edition, Prentice Hall, 2001.

[7] Z.B. Fang, Z.J. Yan, Y.S. Tan, X.Q. Liu and Y.Y. Wang, Appl. Surf. Sci. **241**, 303 (2005).

[8] K.-S. Hwang, Y.-J. Lee and S. Hwangbo, J. Ceram. Proc. Res. **8**, 305 (2007).

[9] T. Matsuda, M. Furuta, T. Hiramatsu, H. Furuta and T. Hirao, J. Vac. Sci. Technol. A **28**, 135 (2010).

[10] J.B. You, X.W. Zhang, Y.M. Fan, Z.G. Yin, P.F. Cai and N.F. Chen, Appl. Surf. Sci. **255**, 5876 (2009).

[11] M.S. Kim, T.H. Kim, D.Y. Kim, G.S. Kim, H.Y. Choi, M.Y. Cho, S.M. Jeon, J.S. Kim, J.S. Kim, D.Y.Lee, J.S.Son, J.I. Lee, J.H. Kim, E. Kim, D.-W. Hwang and J.Y. Leem, J. Crys. Growth **311**, 3568 (2009).

[12] J.-R. Duclère, B. Doggett, M.O. Henry, E. McGlynn, R.T. Rajendra Kumar and J.-P. Mosnier, J. Appl. Phys. **101**, article # 013509 (2007).

[13] J.-R. Duclère, R. O'Haire, A. Meaney, K. Johnston, I. Reid, G. Tobin, J.-P. Mosnier, M. Guilloux-Viry, E. McGlynn and M.O. Henry, J. Mater. Sci.: Mater. Elec. **16**, 421 (2005).

[14] B.-H. Hwang, J. Phys. D: Appl. Phys. **34**, 2469 (2001).

[15] S.B. Newcomb, Inst. Phys. Conf. Ser. **179**, 357 (2004).

[16] R.T. Rajendra Kumar, E. McGlynn, M. Biswas, R. Saunders, G. Trolliard, B. Soulestin, J.-R. Duclere, J.P. Mosnier and M.O. Henry, J. Appl. Phys. **104** article # 084309 (2008).

[17] J. Als-Nielsen and D. McMorrow, Elements of Modern X-Ray Physics, 1st edition reprint, Wiley, 2008.

[18] G. Bauer and W. Richter, Optical Characterization of Epitaxial Semiconductor Layers, 1st edition, Springer,1996.

[19] C. Weidenthaler, Nanoscale **3**, 792 (2011).

[20] R.E. Franklin and R.G. Gosling, Acta Cryst. **6**, 678 (1953).

Tables:

Table 1: Summary of XRD data from samples studied.

Sample identifier	Thickness from spectroscopic ellipsometry (nm; * indicates corroborating TEM measurements)	Integrated Intensity (peak area, arb. units) ZnO (0002) peak	Integrated Intensity (peak area, arb. units) ZnO Si(004) peak	Normalised integrated intensity of ZnO (0002) peak (arb. units)	**Normalised integrated intensity of ZnO (0002) peak per nm film thickness (arb. units)**	FWHM of rocking curve on ZnO (0002) peak (degrees)	***Normalised integrated intensity of ZnO (0002) peak per nm film thickness x (FWHM of rocking curve on ZnO (0002) peak)^2 (arb. units)***
i	33*	3.40E+01	1.48E+05	2.29E-04	6.95E-06	20	2.78E-03
ii	40*	3.00E+01	1.13E+05	2.66E-04	6.64E-06	17.9	2.13E-03
iii	87	1.81E+02	1.64E+05	1.10E-03	1.27E-05	15.35	2.99E-03
iv	339	7.32E+02	1.74E+05	4.20E-03	1.24E-05	13.4	2.22E-03
v	427*	7.77E+03	6.79E+04	1.14E-01	2.68E-04	2.3	1.42E-03
vi	650	1.48E+03	1.13E+05	1.31E-02	2.01E-05	11.25	2.55E-03
vii	761	3.26E+03	1.98E+05	1.65E-02	2.17E-05	8.5	1.57E-03
viii	1057	6.85E+03	1.91E+05	3.58E-02	3.39E-05	7.75	2.04E-03

Figure captions:

Figure 1: (a) XRD diffractograms (note logarithmic y-scale) in 2θ-ω mode on 4 representative ZnO samples, i, ii, v and vi, as listed in table 1; (b) XRD rocking curves on the ZnO (0002) peaks from the samples in (a). In both (a) and (b) different curves are vertically offset for clarity and in (b) the Gaussian fit lines used to determine the curve FWHM are shown by dotted lines (only easily visible for samples i and ii).

Figure 2: Cross-sectional TEM micrographs for the sample labelled (ii) in figure 1 and table 1 shown in a) and b) bright field and c) dark field (imaged using a (10-10) ZnO reflection).

Figure 3: Cross-sectional TEM micrographs for the sample labelled (v) in figure 1 and table 1 shown in a) and b) bright field and c) dark field (imaged using a (10-10) ZnO reflection).

Figure 4: Schematic representations of the ZnO (0002) reciprocal lattice spots (left side) in a textured thin film of constant volume and constant out of plane coherence length for small (a) and large (b) mosaic spreads (shading of the spot indicates the normalized scattering density/intensity) and 2θ-ω and rocking curve scans of the two situations on the right side (with indicative intensity and angular scales for comparative purposes).

Figures:

Figure 1: E. McCarthy *et al*

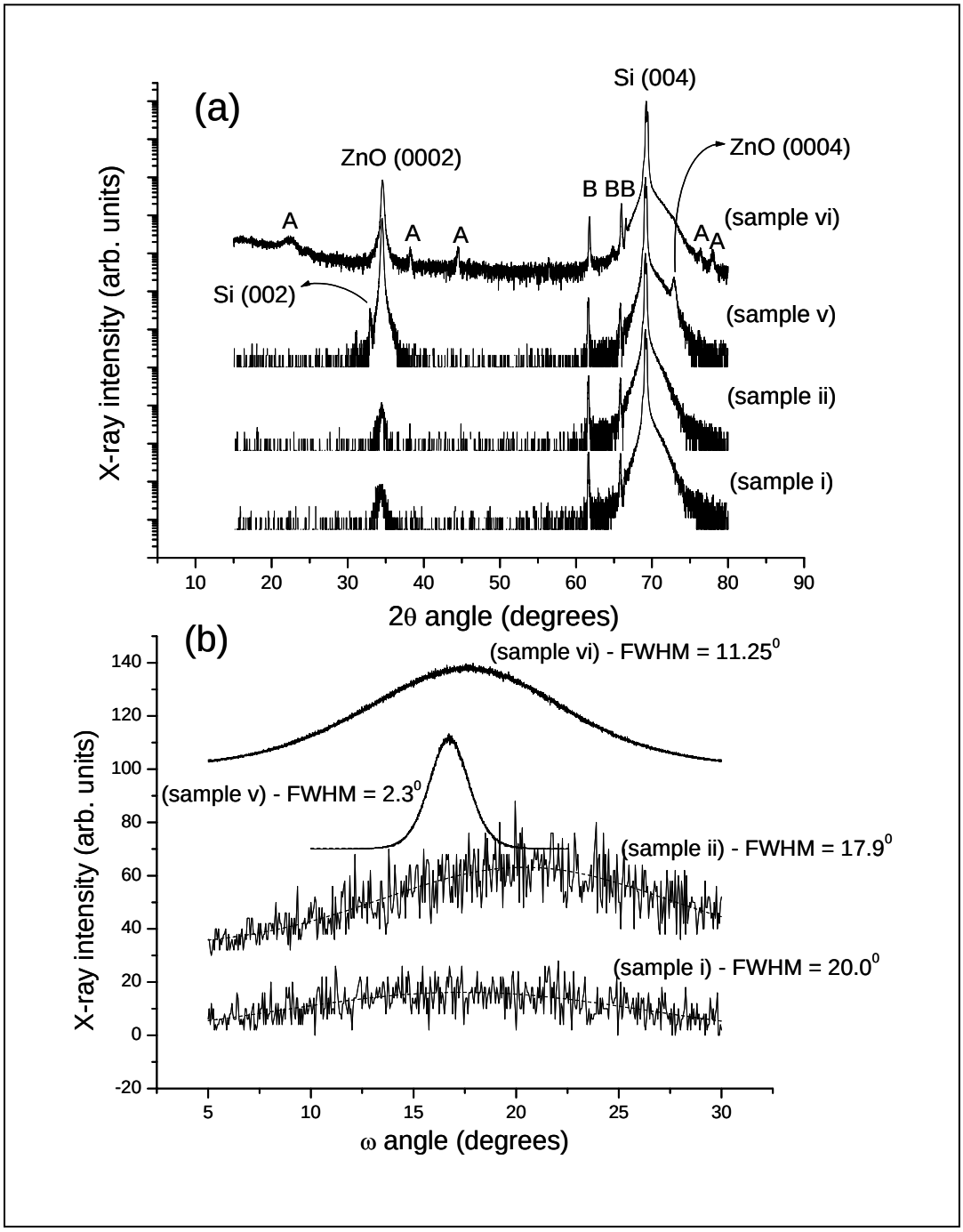

Figure 2: E. McCarthy *et al*

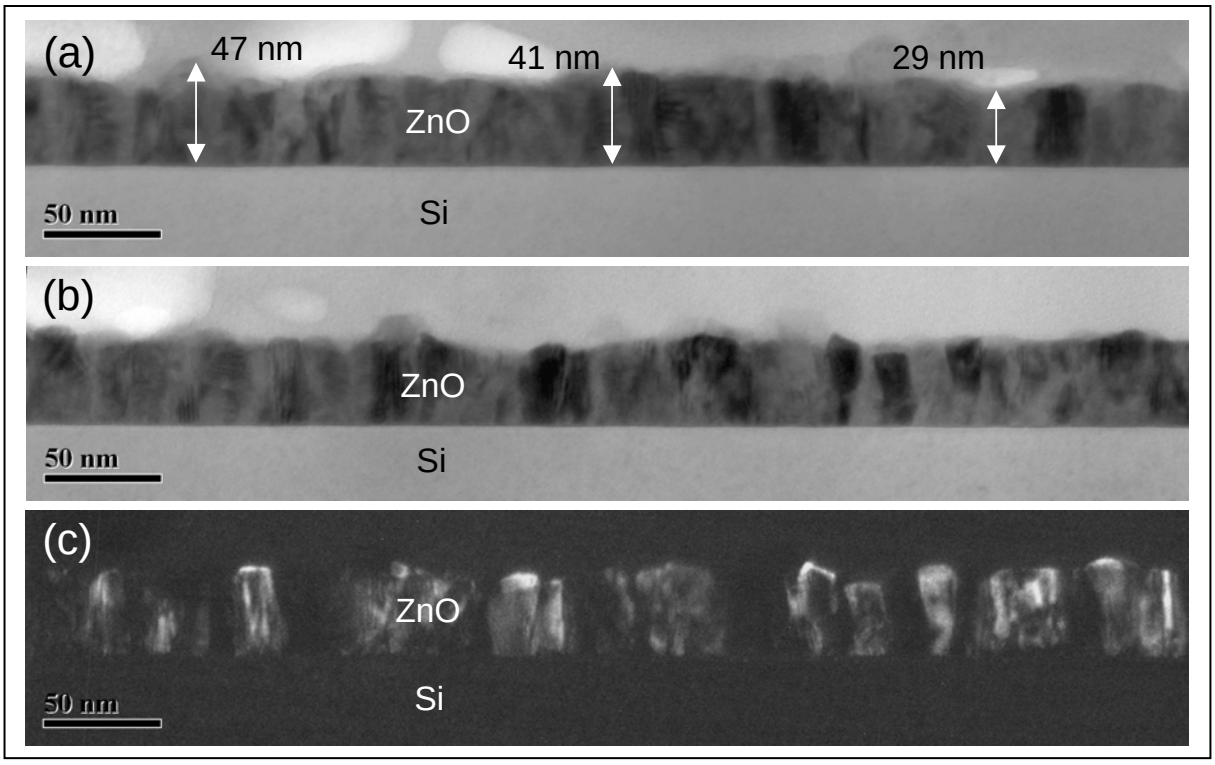

Figure 3: E. McCarthy *et al*

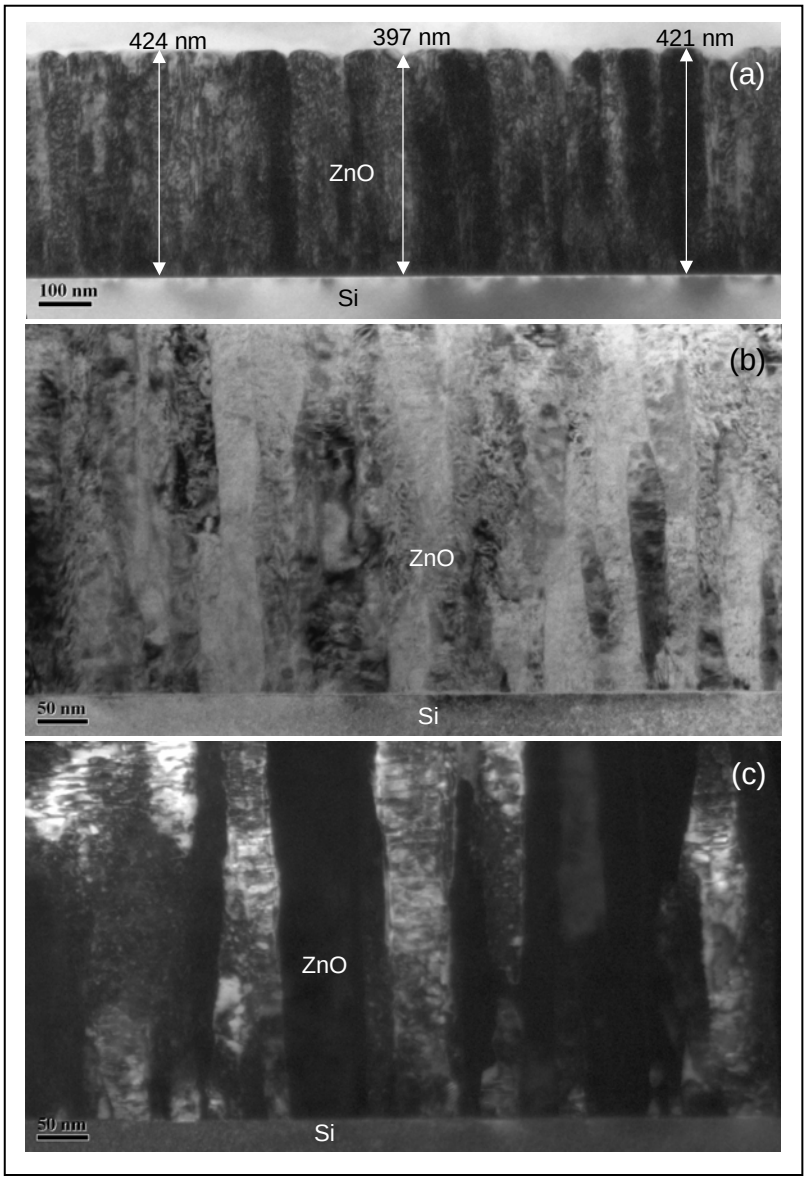

Figure 4: E. McCarthy *et al*